Journal of Materials Science: Materials in Medicine (2020) 31:95
https://doi.org/10.1007/s10856-020-06427-0

BIOCOMPATIBILITY STUDIES

Original Research

Cytotoxicity of bismuth nanoparticles in the murine macrophage cell line RAW 264.7

Jessica Zablocki da Luz[1] · Thiago Neves Machado[2] · Arandi Ginane Bezerra Jr.[2] · Ciro Alberto de Oliveira Ribeiro[1] · Francisco Filipak Neto[1]

Received: 28 April 2020 / Accepted: 24 September 2020 / Published online: 31 October 2020

Abstract

A promising use of bismuth nanoparticles (BiNPs) for different biomedical applications leads to a search for the elucidation of their toxicity mechanisms, since toxicity studies are still at early stage. In the current study, cytotoxic effects of BiNPs produced by laser ablation in solution (LASiS) was investigated in the murine macrophage line RAW 264.7. The cells were exposed to 0.01–50 μg ml^{-1} of BiNPs for 24 and 48 h and then cytotoxicity assays were performed. Decrease of MTT conversion to formazan and of cell attachment were observed with no effects on cell proliferation. No loss of membrane integrity or significant changes of ROS and RNS levels were observed in exposed cells. Foremost, increased phagocytic activity and DNA repair foci occurred for cells exposed to BiNPs. These effects are important findings that must be considered in the case of biomedical application of BiNPs, since inappropriate macrophages activation and inactivation may lead to immunotoxicity.

Graphical Abstract

Bismuth nanoparticles (BiNPs) produced by laser ablation in solution and stabilized with BSA decrease enzyme-dependent MTT conversion to formazan and increase phagocytic activity and DNA repair foci in murine macrophage line RAW 264.7 when exposed to 50 μg ml^{-1}. These effects are findings that should be considered in the case of biomedical application of BiNPs, since inappropriate macrophages activation and inactivation may lead to immunotoxicity.

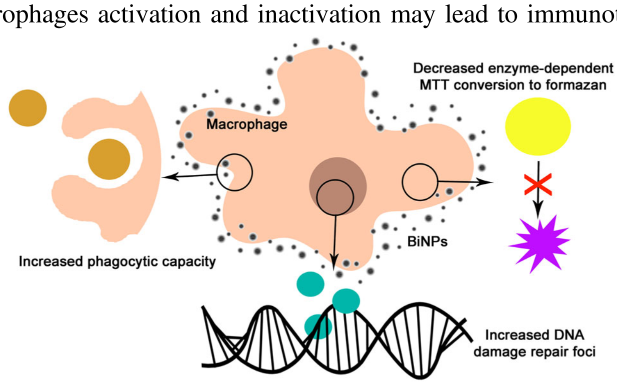

✉ Jessica Zablocki da Luz
jessi_zablocki@ufpr.br

✉ Francisco Filipak Neto
filipak@ufpr.br

1 Laboratório de Toxicologia Celular, Departamento de Biologia Celular, Universidade Federal do Paraná, Curitiba, PR CEP 81.531-990, Brazil

2 Laboratório Fotonanobio, Departamento Acadêmico de Física, Universidade Tecnológica Federal do Paraná, Curitiba, PR CEP 80.230-901, Brazil

1 Introduction

Nanoparticles (NPs) are 1–100 nm range solid materials that have specific physical properties and reactivity as a function of size [1]. Over the past two decades, NPs have been produced industrially in large scale for applications such as electronics, cosmetics, textile industry, and biomedicine [1–4].

According to Nanotechnology Consumer Products Inventory metallic NPs are present in more than 600 products from the 1814 listed products [4]. Among metallic

NPs, bismuth nanoparticles (BiNPs) are very promising, although there is no nanotechnological products in the market [2]. Studies suggest BiNPs can be used for diagnostic imaging (computed tomography), cancer treatment (radiotherapy and thermochemotherapy), drug delivery as nanocarriers and oral antiseptics [5–10]. In addition, BiNPs seem attractive to industry, since they are cheap compared to other metal NPs [11], easily oxidized and dissolved under physiological conditions and thus excreted from the body as soluble molecules [8, 12].

However, decrease of cell viability by disruption of mitochondrial and lysosomal functions in human liver hepatocellular carcinoma (HepG2), normal rat kidney (NRK-52E), Caucasian colon adenocarcinoma (Caco-2) and human alveolar basal epithelial (A549) cells [13] and by autophagy in human embryonic kidney (Hek293) cells [14] were reported when cells were exposed to chemically synthesized BiNPs. Moreover, temporary renal injury in mice, a process linked to autophagy [15] and toxicity in adult *Danio rerio* (zebrafish) fish and eggs [16] were also reported. Therefore, only the study by Reus et al. [17] investigated the toxicity of BiNPs synthesized by physical method. They found that BiNPs are internalized by embryonic mouse fibroblasts (BALB/c 3T3 cells) with concentration-dependent cytotoxic effects and IC50 (half-maximal inhibitory concentration) of ~30 μg ml^{-1}. Thus, a crucial step before applying BiNPs to the biomedical industry is the elucidation of their toxicity mechanisms, since toxicity studies are still in their early stages.

Several NPs may cause immunotoxicity by favoring inflammatory responses and immunosuppression [18]. The immune system is composed of different cell types, including phagocytic cells, such as monocytes, neutrophils, dendritic cells, B cells, and macrophages. These cells can be found in blood, skin, mucous membranes, and in organs such as the liver, spleen, lymph nodes, lung, and brain [18]. Macrophages are mononuclear cells derived from circulating monocytes that reside in tissues and contribute to innate immunity when activated by infectious agents [19]. They secrete inflammatory mediators, process, and present antigens to cells of the adaptive immune system, and act in tissue repair after inflammation [20]. As the first line of defense against infectious agents [21], macrophages represent a very interesting model for immunotoxicity investigation [22]. These cells also express several receptors that facilitate uptake by specific binding to opsonins, being specialized in endocytosis (pinocytosis and phagocytosis), which is considered the main pathway for NPs uptake by cells [23–25].

Thus, the current study aimed to investigate the cytotoxic effects of BiNPs produced by physical method in the murine macrophage line RAW 264.7 using non-specific and macrophage-specific endpoints. This is the first study to investigate the BiNPs toxicity in immune system mammal cells.

2 Materials and methods

2.1 Synthesis and characterization of BiNPs

NPs can be synthesized by chemical and physical methods. Most standard chemical methods produce noxious reductants or require high temperature synthesis, although there are “green” alternatives that combine different techniques to avoid the waste of reactants and are more environmentally sustainable [26]. The physical method by laser ablation in solution (LASiS) produces nanostructures quickly, avoiding waste production and use of chemical reagents, thus also having a reduced environmental impact [27]. Here, BiNPs were synthesized by LASiS, using high-purity bismuth targets (Sigma-Aldrich) immersed in 5 ml of bidistilled water irradiated with the fundamental harmonic of an Nd: YAG Laser (Quantronix 4117, USA) operating at 1064 nm, Q-switched at 1.5 KHz, delivering pulses of 200 ns. A 5-cm focal lens was used to focus the laser beam on the bismuth target for 3 min.

BiNPs tend to aggregate and precipitate ~3 h after synthesis when kept in pure water. One of the strategies used for stabilizing colloidal suspensions is to add some organic molecules to the solution, e.g. bovine serum albumin (BSA), that adsorbs to the NP forming a corona [17, 28, 29]. Therefore, the BiNPs suspension was stabilized with 0.03% BSA shortly after synthesis. Colloidal suspensions of BiNPs were then characterized by UV/Vis spectroscopy (USB2000 + spectrometer, Ocean Optics, USA) and dynamic light scattering (Microtrac Nanotrac Ultra, USA). These techniques allow rapid analysis of the quantity, size, and polydispersity of NPs.

2.2 Cell culture

Aliquots of RAW 264.7 cells (Rio de Janeiro Cell Bank—BCRJ, Rio de Janeiro, RJ, Brazil) were cultured in 25 cm^2 culture flasks with high glucose Dulbecco’s Minimum Essential Medium (DMEM, Cultilab), pH 7.4, with 3700 mg l^{-1} of sodium bicarbonate (MGM). Culture medium was supplemented with 10% FBS (fetal bovine serum, Gibco Invitrogen), 10 μg ml^{-1} streptomycin and 10 U ml^{-1} penicillin (Gibco Invitrogen).

Cells were kept in incubator at 37 °C and 5% pCO_2 for growth and attachment, and subcultures were performed every 48 h, using trypsin (0.5 mg ml^{-1}) and EDTA (ethylenediaminetetraacetic acid, 0.2 mg ml^{-1}, Sigma-Aldrich) for 2–5 min at 37 °C for cell dissociation. For the experiments, the cells were seeded into plates and kept in a CO_2 incubator for 24 h followed by exposure to BiNPs in complete culture medium for 24 and 48 h. For cell viability, cell attachment, reactive nitrogen species (RNS) and reactive oxygen species (ROS) levels assays, 96-well plates were used (24 h: 2×10^4 cells/well; 48 h: 10^4 cells/well). For phagocytic activity and DNA damage assays, 24-well plates with sterilized glass coverslips were used (24 h: 5×10^4 cells/well; 48 h: 2.5×10^4 cells/well). For cell cycle assay, 6-well plates were used (24 h: 2.5×10^5 cells/well and 48 h: 1.5×10^5 cells/well). All reagents used in the procedures were preheated in a water bath at 37 °C.

2.3 Experimental design

Concentrations of BiNPs used for the assays were based on other studies with NPs of Bi compounds [13, 14, 16, 17]. A screening of BiNPs concentrations (0.01, 0.02, 0.05, 0.1, 0.5, 1, 2, 5, 10, 20, and 50 µg ml^{-1}) were performed. Then, four concentrations were selected for further assays (0.05, 0.5, 5, and 50 µg ml^{-1}). The control group received the complete culture medium with bidistilled water and BSA. Three independent experiments using different cryopreserved cell vials were performed.

2.4 Non-specific cytotoxicity assays

2.4.1 Cell viability

Plasma membrane integrity assay: after exposure, the cells were incubated with 50 µl of trypan blue (Sigma-Aldrich) for 1 min, washed with phosphate-buffered saline (PBS) and 3–4 images were captured per well under an inverted light microscope (Leica Microsystems, Germany). A minimum of 100 cells per image were classified as viable or nonviable in a total of ten images per group and experiment.

MTT conversion assay: after exposure, the cells were incubated with 200 µl of MTT solution (3-(4,5-dimethylthiazol-2-yl)-2,5-diphenyltetrazolium bromide), 0.5 mg ml^{-1}, Amresco) in culture medium for 2 h in the CO_2 incubator and washed twice with PBS. Intracellular formazan crystals were dissolved in 100 µl DMSO (dimethyl sulfoxide, Synth) per well and absorbance was determined on microplate spectrophotometer (BioTek Epoch, USA) using 550 nm wavelength.

2.4.2 Cell attachment

After exposure, the cells were washed once with PBS, fixed with 100 µl of methanol (Neon) for 15 min and stained with 100 µl of violet crystal (0.25 mg ml^{-1}, Certistain) for 10 min at room temperature. The cells were washed twice with 150 µl of distilled water and the stain was extracted with 100 µl of 33% acetic acid (Neon) for 30 min at room temperature and shaking. Finally, the absorbance was determined in a microplate spectrophotometer (BioTek Epoch, USA) using 570 nm wavelength.

2.4.3 DNA damage

After exposure, the cells were fixed with 4% paraformaldehyde (Sigma-Aldrich) in PBS for 30 min, permeabilized with 0.2% Triton-X in PBS for 10 min, washed once with PBS and incubated with mouse anti-phospho-H2AX conjugated with Alexa Fluor 488 (1:100, eBioscience) for 2 h and DAPI (4′,6-diamidino-2-phenylindole, 5 µg ml^{-1}, Sigma-Aldrich) for 10 min. The coverslips were mounted on Fluormount resin and then four images per group and experiment were captured in a confocal microscope (Nikon Eclipse Ti microscope, Japan). Approximately 100 nuclei per group and independent experiment were classified as labeled or unlabeled.

2.4.4 Cell cycle

After exposure, the cells were trypsinized, removed to microtubes, fixed in 70% ethanol (Neon) for 2 h, washed twice with PBS and resuspended with 0.5 ml of staining buffer (fetal bovine serum 2% in PBS) with propidium iodide and RNase enzyme (BD Pharmigen). The cells were analyzed in flow cytometer (Accuri C6 Plus, BD Biosciences, USA) with acquisition of 10,000 gated events.

2.5 Specific cytotoxicity assays

Assays related to specific phagocytic cell functions, such as the phagocytic activity assay and the levels of ROS and RNS, were also performed in RAW 264.7 cells.

2.5.1 Phagocytic activity

After exposure, the culture medium was replaced by 1 ml fetal bovine serum-free fresh medium containing of *Saccharomyces cerevisiae* yeasts (2×10^6 cells/ml, ~10 yeasts/ macrophage). After 2 h incubation, the cells were washed with PBS, fixed in 95% ethanol for 5 min at room temperature, stained with 20% Giemsa stain (Merck) for 5 min. Then, the coverslips were rapidly dehydrated in ethanol series and xylene (Anidrol) and mounted on glass slides with Permount resin. For the analysis, images were captured on a slide scanner (Metafer V3.9, Zeiss, Germany) and the total number of macrophages (A), number of macrophages with internalized yeast (B) and the number of internalized yeast (C) were counted. The phagocytic activity was calculated according to Buchi et al. [30] by the formula $(C/B) \times (B/A)$, using data of 100 macrophages per group and experiment.

2.5.2 ROS and RNS levels

ROS: after exposure, the cells were incubated with 10 µM of 2′,7′-dichlorodihydrofluorescein diacetate (DCF, Thermo Fisher) in culture medium for 15 min at 37 °C (protected from

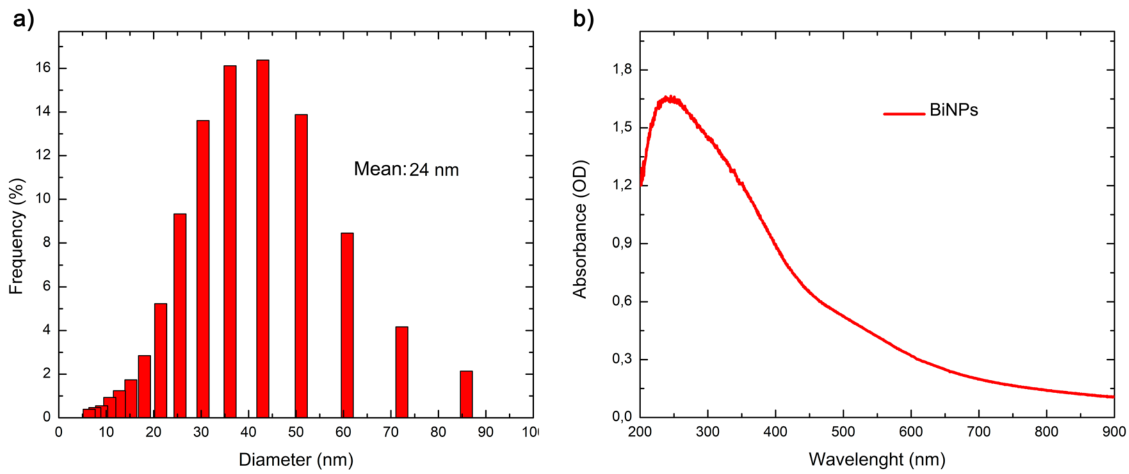

Fig. 1 Characterization of BiNPs colloidal suspensions by UV/Vis spectroscopy (**a**) and dynamic light scattering (**b**). BiNPs had a wide size distribution from 4 to 87 nm, with a high prevalence (~80%) at 25–60 nm range (**a**), and a peak absorption at 250 nm wavelength (**b**)

light), and washed twice with PBS. Fluorescence was measured in a spectrofluorometer (Infinite M200, Tecan, Switzerland) using 488/530 nm (excitation/emission) wavelength.

RNS: after exposure, the culture medium were transferred to a black microplate and 10 µl of 2,3-diaminonaphthalene (DAN, 0.5 mg ml^{-1}, Invitrogen) in 0.62 M of hydrochloride acid (HCl) were added. The microplates were incubated at 25 °C (protected from light) for 30 min under gentle shaking, and 5 µl of 2.8 M of sodium hydroxide (NaOH) was added. The formation of 1-naphthotriazole derived from the reaction of nitrite and 2,3-diaminonaphthalene was determined by fluorescence measurement (Infinite M200, Tecan, Switzerland) using 365/450 nm (excitation/emission) wavelength.

2.6 Statistical analysis

Three independent experiments were performed for all the assays. The average value of subsamples per group were calculated in each independent experiment and used for statistical comparisons ($N = 3$). Data was analyzed through Kruskal–Wallis test followed by Dunn's multiple comparison posttest (nonparametric), comparing the exposed groups versus the control. Differences were considered significant when p values were < 0.05.

3 Results

3.1 BiNPs are heterogeneous in size

BiNPs synthesized by laser ablation had a wide size distribution from 4 to 87 nm, with a high prevalence (~80%) at 25–60 nm range (Fig. 1a), and a peak absorption at 250 nm wavelength (Fig. 1b). NP suspensions in 0.03% BSA were stable for more than 30 days, with no precipitation and agglomeration.

3.2 Cell viability and attachment decreased after exposure to BiNPs

No effects were observed for cells exposed to BiNPs for 24 h (Fig. 2a–e). However, exposure to BiNPs for 48 h led to decreases of cell viability observed through a concentration-dependent decrease of the conversion of MTT to formazan for 20 (45%) and 50 µg ml^{-1} (64%) of BiNPs (Fig. 2b), and through decreased cell attachment (18%) for 50 µg ml^{-1} of BiNPs (Fig. 2f). Plasma membrane integrity assay was generally not efficient to detect the decreases of cell viability for 24 h (Fig. 2c) and 48 h (Fig. 2d) of exposure. In addition, there was no alteration in the distribution of cells in the cell cycle phases after exposure to BiNPs for 24 h (Fig. 2g) and 48 h (Fig. 2h).

3.3 BiNPs exposure led to increased phagocytic activity with slight alterations of ROS and RNS levels

The phagocytic activity increased in the cells were exposed for 24 h (~210%) and 48 h (~90%) to 50 µg ml^{-1} of BiNPs (Fig. 3e–g). ROS and RNS levels were not altered for the cells exposed to BiNPs for 24 h (Fig. 3a–c). However, 48 h exposure led to an increase (~60%) of ROS levels at 5 µg ml^{-1} of BiNPs (Fig. 3b) and decrease (~30%) of RNS levels at 50 µg ml^{-1} (Fig. 3d).

3.4 DNA damage repair foci increased after exposure to BiNPs

The number of nuclei with positive repair foci (phospho-H2AX positive) increased in the cells exposed to 50 µg ml^{-1} of BiNPs for 24 h (~15%) and 48 h (~30%) (Fig. 4a, b).

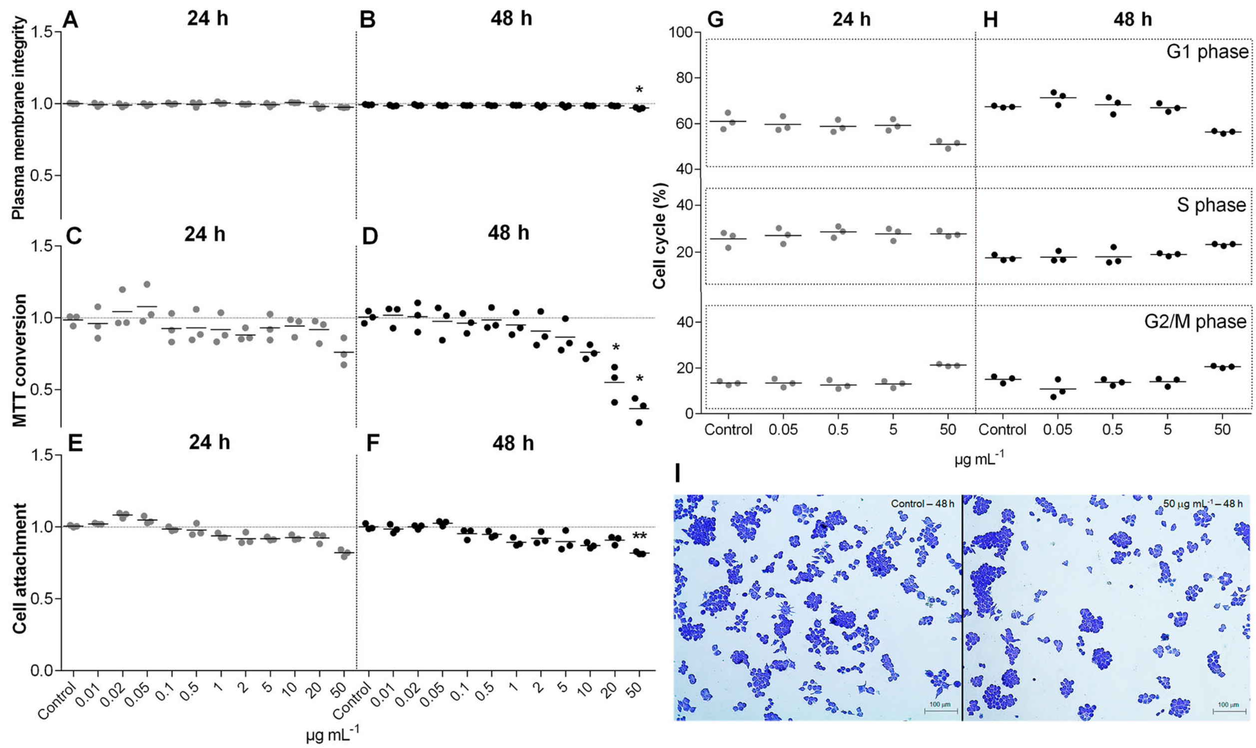

Fig. 2 Effects of BiNPs on cell viability (**a–d**), cell attachment (**e**, **f**), and cell cycle (**g**, **h**). Exposure to BiNPs for 48 h led to decreases of cell viability observed through a concentration-dependent decrease of the conversion of MTT to formazan for 20 (45%) and 50 µg ml^{-1} (64%) of BiNPs (**b**) and through decrease of the cell attachment (18%) for 50 µg ml^{-1} of BiNPs (**f**, **i**). Images of attached cells stained with crystal violet under light microscopy (**i**). *$p < 0.05$

4 Discussion

In the current study, we observed that BiNPs synthesized by laser ablation were toxic to RAW 264.7 murine macrophage line after 24 and 48 h exposure, but effects occurred mostly at a high concentration (50 µg ml^{-1}). In general, cell viability and attachment decreased, DNA damage repair foci and phagocytic activity increased with only slight alterations of ROS and RNS levels. Such a concentration may not be achieved by environmental exposure, but attention may be paid in the case of potential use of BiNPs for biomedical applications such as diagnostic imaging and cancer treatment. In studies suggesting the use of BiNPs for cancer treatment, the concentrations tested were similar to those tested in the current study. Concentrations of 5–100 µg ml^{-1} have been used for in vitro assays [7, 8] and mice have been intravenously injected with 100 µl of 4 mg ml^{-1} NPs (final dose of 20 µg g^{-1}) [8] in in vivo approaches.

Cell viability and attachment decreased after exposure to BiNPs, particularly after 48 h exposure. Abudayyak et al. [13] found concentration-dependent decreases of MTT conversion for Bi_2O_3 NPs in HepG2, NRK-52E, Caco-2, and A549 cell lines exposed to concentrations from 1 to 100 µg ml^{-1} for 24 h. In general, toxicity is highly dependent on cell type. For example, Liu et al. [29] found 78% decrease of MTT conversion in A549 lung cells at 160 µg ml^{-1} and 80% decrease in HEK293 at 20 µg ml^{-1} of BiNPs. The authors pointed out that this renal cell toxicity may also be due to bismuth ions or combined effect of the suspension ions and BiNPs. RAW 264.7 cells were somewhere in between these two cell types, with a 64% decrease of MTT conversion at 50 µg ml^{-1} of BiNPs.

One important observation is that MTT assay was more sensitive to detect BiNPs cytotoxicity in RAW 264.7 cells than trypan blue exclusion assay. Sabella et al. [31] described a general mechanism by which metallic NPs generate cytotoxicity. NPs are uptaken by endocytosis and directed to lysosomes, where the acidic condition promotes the release of ions that exert toxicity by interacting with proteins, resulting in damage to organelles, increased levels of ROS and, ultimately, DNA and plasma membrane damage. In addition, we cannot ignore the fact that complete rupture of cells can lead to underestimation of non-viable cell counting in trypan blue assay, as well as decrease the absorbance in crystal violet assay used for cell attachment assay. Moreover, Bi ions may also contribute to the cytotoxicity observed. In addition to a very small presence of ions in the colloidal suspension, BiNPs may be uptaken by the cells through endocytosis and directed to lysosomes, as previously mentioned, where the acidic condition

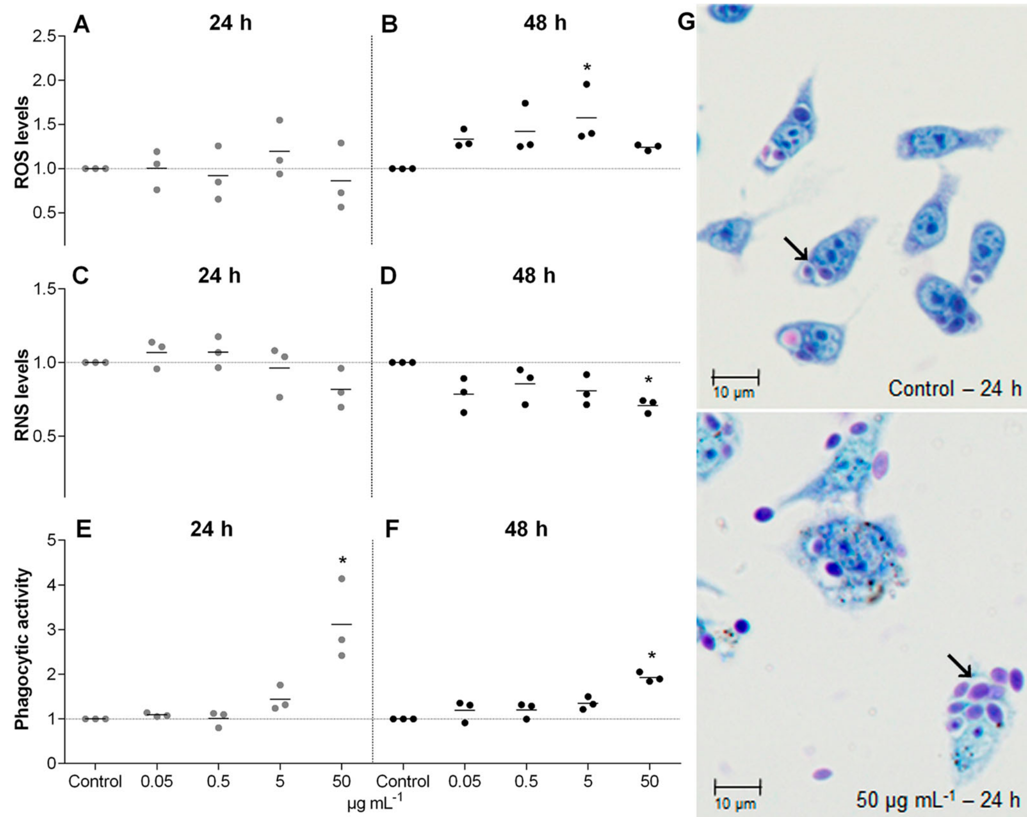

Fig. 3 Effects of BiNPs on ROS levels (**a**, **b**), RNS levels (**c**, **d**), and phagocytic activity (**e**, **f**). The phagocytic activity increased in the cells were exposed for 24 h (~210%) and 48 h (~90%) to 50 µg ml^{-1} of BiNPs (**e**–**g**). Macrophages with internalized yeasts (**g**, arrow) under light microscopy (Giemsa stain). *$p < 0.05$

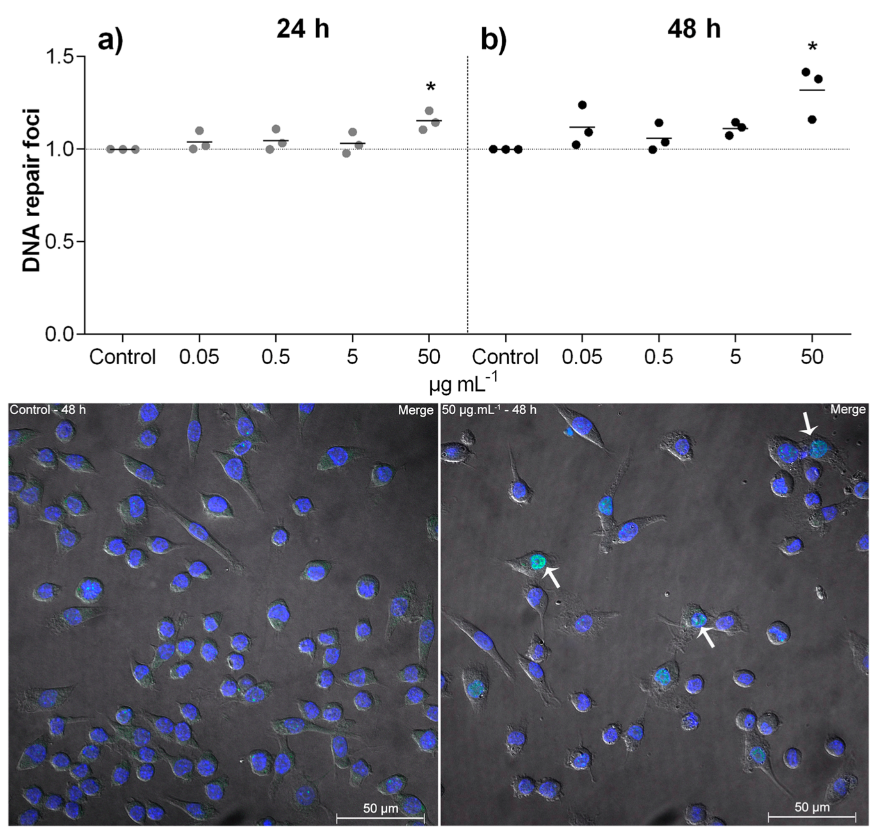

Fig. 4 Effects of BiNPs on DNA damage (**a**, **b**). The number of nuclei with positive repair foci (phospho-H2AX positive) increased in the cells were exposed to 50 µg ml^{-1} of BiNPs for 24 h (~15%) and 48 h (~30%) (**a**, **b**). Macrophages labeled with DAPI (nuclei in blue) and anti-phospho-H2AX (positive labeling for repair foci in green) under confocal microscopy. Light blue represents the overlap of blue and green labeling. *$p < 0.05$

promotes the release of ions that also exert toxicity [31]. Therefore, as for most metallic NPs, it is not possible to distinguish whether the effects are caused directly by NPs themselves or indirectly by the ions released inside the cells by NPs dissolution. We think that the effects are probably a combination of both.

Decrease of the number of attached cells occurred for RAW 264.7 cells exposed to BiNPs, which is not related to a decrease of cell proliferation, since there were no changes on the distribution profile in the cell cycle phases, although DNA repair foci increased. Indeed, control mechanisms can generate a transient delay of cell cycle to guarantee appropriate DNA repair and genomic stability, thereby decreasing the proliferation rate [32]. Decrease of cell attachment may interfere with the immune response and have been reported for other metallic NPs such as gold, silver, and titanium dioxide. Wei et al. [33] observed that gold NPs cause loss of cell attachment in HepG2 cells and Peng et al. [34] reported that several metallic NPs cause loss of cell attachment by preventing vascular endothelial (VE)–cadherin/VE–cadherin interactions in human microvascular endothelial tissue cells.

DNA damage repair foci also increased in RAW 264.7 cells after 24 and 48 h exposure to BiNPs at $50\,\mu g\,ml^{-1}$. Many mechanisms can lead to DNA damage, but for chemical stress the redox unbalance is one of the most common. Free radicals, such as hydroxyl radical and singlet oxygen can oxidize cell biomolecules, causing oxidative modifications in DNA, such as double-strand breaks and oxidation of nitrogenous bases [35]. As only a slight increase of intracellular ROS levels was observed for cells exposed to $5\,\mu g\,ml^{-1}$, either DNA damage is being caused by ROS production in specific cell compartments or other mechanisms are involved. In addition, we measured only intracellular ROS levels using DCF fluorescence, and phagocytes such as macrophages express high levels of the enzyme NADPH oxidase (nicotinamide adenine dinucleotide phosphate oxidase), which produces ROS extracellularly. Other studies also have shown that metallic NPs can cause DNA damage. Hashimoto et al. [36] observed that aluminum oxide NPs cause DNA damage in RAW 264.7 cells and reported that these effects were mainly due to the interaction of these NPs with cell organelles, but also could be due to direct interaction of the NPs with DNA. Nguyen et al. [37] observed increase of 8-hydroxy-2′-deoxyguanosine (8-OHdG) levels, the most common marker of oxidative DNA damage, in J774A.1 (mouse BALB/c) monocytes exposed to silver NPs. Considering these findings and the importance of determining the mutagenic potential of BiNPs, further research of the issue is necessary.

Another important effect of BiNPs in RAW 264.7 cells observed in this study was the increase of phagocytic activity, which may interfere with the immune system response in vivo. Similar results have been reported for other metallic NPs. Wang et al. [38] observed through in vivo (intranasal exposure in mice) and in vitro (BV-2 cells) approaches that microglia exposed to iron oxide NPs had increased phagocytic activity. Chen et al. [39] observed that RAW 264.7 cells and primary cultured macrophages derived from mice bone marrow had increased *E. coli* phagocytosis and protein-positive regulation of the complement system proteins (proteomic analysis) when exposed to titanium dioxide NPs. Thus, there is strong evidence that some metallic NPs increase the phagocytic activity of macrophages, although the exact mechanisms have not been described. Macrophages initiate phagocytosis by identifying molecular patterns associated with the pathogen surface through pattern recognition receptors, which include lectins, mannose receptor, Toll-like receptors (TLRs), and Fcγ receptor. TLR4, a member of the TLR family, plays a critical role in pathogen detection and triggering immune responses by initiating signal transduction [40]. Nuclear factor-κB (NF-κB) protein complex and mitogen-activated protein kinase are key elements related to proinflammatory signaling, and NF-κB is an evolutionarily conserved transcription factor that modulates the expression of various genes involved in immune responses [40]. As both signaling pathways are considered to be involved in phagocytosis, BiNPs could also be interfering with these pathways in RAW 264.7 cells. Additionally, the increase of macrophage activity is an important finding as an immune activation process may favor the development of tissue damage and chronic disease [41].

Several studies report an inverse relation between toxicity and size of other NPs [42, 43]. Depending on the size of the NP, it can penetrate membranes of different cell compartments, which is also related to cytotoxicity [43]. For example, gold NPs no larger than 6 nm enter the cell nucleus, whereas large NPs (10 or 16 nm) penetrate through the cell membrane and are found only in the cytoplasm [44]. Moreover, larger gold and silver NPs have been found to be less toxic than smaller ones for several cells lines [45, 46]. The BiNPs used to the current study had a wide size distribution range, typical for laser ablation-produced NPs, as monodisperse suspensions are possible but difficult to achieve [47]. Thus, the responses observed in macrophages exposed to BiNPs may have been due to different toxicity mechanisms, which vary depending on the size of the NPs [48]. In addition, the BiNPs synthesized by the Fotonanobio laboratory had spherical format and zeta potential of +39 mV in water and −23 mV in the presence of BSA [17, 47, 49]. Apparently, the formation of an organic corona of albumin is necessary for the stability of BiNPs [17] and the reduction of the zeta potential may influence their toxicity for RAW 264.7 cells, since phagocytic cells preferentially interact with negatively charged particles unlike non-phagocytic cells [50].

5 Conclusion

This study showed the toxic potential of BiNPs to RAW 264.7 macrophages. In particular, the decreases of enzyme-dependent MTT conversion to formazan, cell attachment, and foremost the increases of DNA damage repair foci and phagocytic capacity are important findings that must be considered in the case of biomedical application of BiNPs and should be better investigated, since inappropriate activation and inactivation of macrophages may lead to immunotoxicity.

Acknowledgements This research was supported by CNPq (National Council for Scientific and Technological Development, scholarship) and Fundação Araucária de Apoio ao Desenvolvimento Científico e Tecnológico do Paraná (Research Foundation of Parana State, research funding, Convênio FA-UFPR 006/2017).

Compliance with ethical standards

Conflict of interest JZdL has received Scholarship (master's course) from CNPq (National Council for Scientific and Technological Development). AGB has received financial support from CNPq (National Council for Scientific and Technological Development). FFN has received financial support for the project from Fundação Araucária de Apoio ao Desenvolvimento Científico e tecnológico do Paraná (Research Foundation of Parana State).

Publisher's note Springer Nature remains neutral with regard to jurisdictional claims in published maps and institutional affiliations.

References

1. Madden AS, Hochella MF, Jr. A test of geochemical reactivity as a function of mineral size: manganese oxidation promoted by hematite nanoparticles. Geochim Cosmochim Acta. 2005;69:389–98. https://doi.org/10.1016/j.gca.2004.06.035.
2. The Project on Emerging Nanotechnologies. 2019. http://www.nanotechproject.org. Accessed 7 May 2016.
3. EPA. Nanotechnology White Paper. US Enviromental Protection Agency Report EPA 100/B-07/001. Washington; 2007. http://www.epa.gov. Accessed 7 June 2016.
4. Vance ME, Kuiken T, Vejerano EP, McGinnis SP, Hochella MF, Rejeski D, et al. Nanotechnology in the real world: redeveloping the nanomaterial consumer products inventory. Beilstein J Nanotechnol. 2015;6:1769–80. https://doi.org/10.3762/bjnano.6.181.
5. Keogan DM, Griffith DM. Current and potential applications of bismuth-based drugs. Molecules. 2014;19:15258–97. https://doi.org/10.3390/molecules190915258.
6. El-Batal AI, El-Sayyad GS, El-Ghamry A, Agaypi KM, Elsayed MA, Gobara M. Melanin-gamma rays assistants for bismuth oxide nanoparticles synthesis at room temperature for enhancing antimicrobial, and photocatalytic activity. J Photochem Photobio B. 2017;173:120–39. https://doi.org/10.1016/j.jphotobiol.2017.05.030.
7. Stewart C, Konstantinov K, McKinnon S, Guatelli S, Lerch M, Rosenfeld A, et al. First proof of bismuth oxide nanoparticles as efficient radiosensitisers on highly radioresistant cancer cells. Phys Med. 2016;32:1444–52. https://doi.org/10.1016/j.ejmp.2016.10.015.
8. Deng J, Xu S, Hu W, Xun X, Zheng L, Su M. Tumor targeted, stealthy and degradable bismuth nanoparticles for enhanced X-ray radiation therapy of breast cancer. Biomaterials 2018;154:24–33. https://doi.org/10.1016/j.biomaterials.2017.10.048.
9. Hernandez-Delgadillo R, Del Angel-Mosqueda C, Solís-Soto JM, Munguia-Moreno S, Pineda-Aguilar N, Sánchez-Nájera RI, et al. Antimicrobial and antibiofilm activities of MTA supplemented with bismuth lipophilic nanoparticles. Dent Mater J. 2017;36:503–10. https://doi.org/10.4012/dmj.2016-259.
10. Hernandez-Delgadillo R, Velasco-Arias D, Martinez-Sanmiguel JJ, Diaz D, Zumeta-Dube I, Arevalo-Niño K, et al. Bismuth oxide aqueous colloidal nanoparticles inhibit Candida albicans growth and biofilm formation. Int J Nanomed. 2013;8:1645–52. https://doi.org/10.2147/ijn.s38708.
11. Cabral-Romero C, Shankararaman C. Bismuth nanoparticles: antimicrobials of broad-spectrum, low cost and safety. Nanomedicine. 2014;17:430–8.
12. Brown AL, Goforth AM. pH-Dependent synthesis and stability of aqueous, elemental bismuth glyconanoparticle colloids: potentially biocompatible X-ray contrast agents. Chem Mater. 2012;24:1599–605. https://doi.org/10.1021/cm300083j.
13. Abudayyak M, Öztaş E, Arici M, Özhan G. Investigation of the toxicity of bismuth oxide nanoparticles in various cell lines. Chemosphere. 2017;169:117–23. https://doi.org/10.1016/j.chemosphere.2016.11.018.
14. Liu Y, Zhuang J, Zhang X, Yue C, Zhu N, Yang L, et al. Autophagy associated cytotoxicity and cellular uptake mechanisms of bismuth nanoparticles in human kidney cells. Toxicol Lett. 2017;275:39–48. https://doi.org/10.1016/j.toxlet.2017.04.014.
15. Liu Y, Yu H, Zhang X, Wang Y, Song Z, Zhao J, et al. The protective role of autophagy in nephrotoxicity induced by bismuth nanoparticles through AMPK/mTOR pathway. Nanotoxicology. 2018;12:586–601. https://doi.org/10.1080/17435390.2018.1466932.
16. Kovrižnych JA, Sotníková R, Zeljenková D, Rollerová E, Szabová E, Wimmerová S. Acute toxicity of 31 different nanoparticles to zebrafish (Danio rerio) tested in adulthood and in early life stages—comparative study. Interdiscip Toxicol. 2013;6:67–73. https://doi.org/10.2478/intox-2013-0012.
17. Reus TL, Machado TN, Bezerra AG, Marcon BH, Paschoal ACC, Kuligovski C, et al. Dose-dependent cytotoxicity of bismuth nanoparticles produced by LASiS in a reference mammalian cell line BALB/c 3T3. Toxicol Vitr. 2018;53:99–106. https://doi.org/10.1016/j.tiv.2018.07.003.
18. Pandey RK, Prajapati VK. Molecular and immunological toxic effects of nanoparticles. Int J Biol Macromol. 2018;107:1278–93. https://doi.org/10.1016/j.ijbiomac.2017.09.110.
19. Kato K, Yamamoto K, Okuyama H, Kimura T. Microbicidal activity and morphological characteristics of lung macrophages in Mycobacterium bovis BCG cell wall-induced lung granuloma in mice. Infect Immun. 1984;45:325–31.
20. Granata F, Frattini A, Loffredo S, Del Prete A, Sozzani S, Marone G, et al. Signaling events involved in cytokine and chemokine production induced by secretory phospholipase A2 in human lung macrophages. Eur J Immunol. 2006;36:1938–50. https://doi.org/10.1002/eji.200535567.
21. Babior BM. Phagocytes and oxidative stress. Am J Med. 2000;109:33–44.
22. Descotes J. Importance of immunotoxicity in safety assessment: a medical toxicologist's perspective. Toxicol Lett. 2004;149:103–8. https://doi.org/10.1016/j.toxlet.2003.12.024.
23. Rejman J, Oberle V, Zuhorn IS, Hoekstra D. Size-dependent internalization of particles via the pathways of clathrin- and caveolae-mediated endocytosis. Biochem J. 2004;377:159–69. https://doi.org/10.1042/bj20031253.
24. Hillaireau H, Couvreur P. Nanocarriers' entry into the cell: relevance to drug delivery. Cell Mol Life Sci. 2009;66:2873–96. https://doi.org/10.1007/s00018-009-0053-z.

25. Ferreira LA, Radaic A, Pugliese GO, Valentini MB, Oliveira MR, de Jesus JM. Endocitose e tráfego intracelular de nanomateriais. Acta Farmacêutica Portuguesa. 2014;3:143–54.
26. Reverberi AP, Varbanov PS, Lauciello S, Salerno M, Fabiano B. An eco-friendly process for zerovalent bismuth nanoparticles synthesis. J Clean Prod. 2018;198:37–45. https://doi.org/10.1016/j.jclepro.2018.07.011.
27. Barcikowski S, Compagnini G. Advanced nanoparticle generation and excitation by lasers in liquids. Phys Chem Chem Phys. 2013;15:3022–6. https://doi.org/10.1039/c2cp90132c.
28. Wu X, He X, Wang K, Xie C, Zhou B, Qing Z. Ultrasmall near-infrared gold nanoclusters for tumor fluorescence imaging in vivo. Nanoscale. 2010;2:2244–9. https://doi.org/10.1039/c0nr00359j.
29. Liu Y, Zhuang J, Zhang X, Yue C, Zhu N, Yang L, et al. Autophagy associated cytotoxicity and cellular uptake mechanisms of bismuth nanoparticles in human kidney cells. Toxicol Lett. 2017;275:39–48. https://doi.org/10.1016/j.toxlet.2017.04.014.
30. Buchi DdF, Souza W. Internalization of surface components during ingestion of Saccharomyces cerevisiae by macrophages. J Submicroscopic Cytol Pathol. 1992;24:135–41.
31. Sabella S, Carney RP, Brunetti V, Malvindi MA, Al-Juffali N, Vecchio G, et al. A general mechanism for intracellular toxicity of metal-containing nanoparticles. Nanoscale. 2014;6:7052–61. https://doi.org/10.1039/c4nr01234h.
32. Shackelford RE, Kaufmann WK, Paules RS. Cell cycle control, checkpoint mechanisms, and genotoxic stress. Environ Health Perspect. 1999;107:5–24. https://doi.org/10.1289/ehp.99107s15.
33. Wei XL, Mo ZH, Li B, Wei JM. Disruption of HepG2 cell adhesion by gold nanoparticle and Paclitaxel disclosed by in situ QCM measurement. Colloids Surf B Biointerfaces. 2007;59:100–4. https://doi.org/10.1016/j.colsurfb.2007.04.016.
34. Peng F, Setyawati MI, Tee JK, Ding X, Wang J, Nga ME, et al. Nanoparticles promote in vivo breast cancer cell intravasation and extravasation by inducing endothelial leakiness. Nat Nanotechnol. 2019. https://doi.org/10.1038/s41565-018-0356-z.
35. Wan R, Mo Y, Feng L, Chien S, Tollerud DJ, Zhang Q. DNA damage caused by metal nanoparticles: involvement of oxidative stress and activation of ATM. Chem Res Toxicol. 2012;25:1402–11. https://doi.org/10.1021/tx200513t.
36. Hashimoto M, Imazato S. Cytotoxic and genotoxic characterization of aluminum and silicon oxide nanoparticles in macrophages. Dent Mater. 2015;31:556–64. https://doi.org/10.1016/j.dental.2015.02.009.
37. Nguyen KC, Richards L, Massarsky A, Moon TW, Tayabali AF. Toxicological evaluation of representative silver nanoparticles in macrophages and epithelial cells. Toxicol Vitr. 2016;33:163–73. https://doi.org/10.1016/j.tiv.2016.03.004.
38. Wang Y, Wang B, Zhu M-T, Li M, Wang H-J, Wang M, et al. Microglial activation, recruitment and phagocytosis as linked phenomena in ferric oxide nanoparticle exposure. Toxicol Lett. 2011;205:26–37. https://doi.org/10.1016/j.toxlet.2011.05.001.
39. Chen Q, Wang N, Zhu M, Lu J, Zhong H, Xue X, et al. TiO2 nanoparticles cause mitochondrial dysfunction, activate inflammatory responses, and attenuate phagocytosis in macrophages: a proteomic and metabolomic insight. Redox Biol. 2018;15:266–76. https://doi.org/10.1016/j.redox.2017.12.011.
40. Bi D, Zhou R, Cai N, Lai Q, Han Q, Peng Y, et al. Alginate enhances Toll-like receptor 4-mediated phagocytosis by murine RAW264.7 macrophages. Int J Biol Macromol. 2017;105:1446–54. https://doi.org/10.1016/j.ijbiomac.2017.07.129.
41. Laskin DL, Sunil VR, Gardner CR, Laskin JD. Macrophages and tissue injury: agents of defense or destruction? Annu Rev Pharm Toxicol. 2011;51:267–88. https://doi.org/10.1146/annurev.pharmtox.010909.105812.
42. Bahadar H, Maqbool F, Niaz K, Abdollahi M. Toxicity of nanoparticles and an overview of current experimental models. Iran Biomed J. 2016;20:1–11.
43. Sukhanova A, Bozrova S, Sokolov P, Berestovoy M, Karaulov A, Nabiev I. Dependence of nanoparticle toxicity on their physical and chemical properties. Nanoscale Res Lett. 2018;13:44. https://doi.org/10.1186/s11671-018-2457-x.
44. Huo S, Jin S, Ma X, Xue X, Yang K, Kumar A, et al. Ultrasmall gold nanoparticles as carriers for nucleus-based gene therapy due to size-dependent nuclear entry. ACS Nano. 2014;8:5852–62. https://doi.org/10.1021/nn5008572.
45. Pan Y, Neuss S, Leifert A, Fischler M, Wen F, Simon U, et al. Size-dependent cytotoxicity of gold nanoparticles. Small. 2007;3:1941–9. https://doi.org/10.1002/smll.200700378.
46. Perde-Schrepler M, Florea A, Brie I, Virag P, Fischer-Fodor E, Vâlcan A, et al. Size-Dependent cytotoxicity and genotoxicity of silver nanoparticles in cochlear cells in vitro. J Nanomaterials. 2019;2019:6090259. https://doi.org/10.1155/2019/6090259.
47. Bezerra AG, Cavassin P, Machado TN, Woiski TD, Caetano R, Schreiner WH. Surface-enhanced Raman scattering using bismuth nanoparticles: a study with amino acids. J Nanopart Res. 2017;19:362. https://doi.org/10.1007/s11051-017-4057-6.
48. Shang L, Nienhaus K, Nienhaus GU. Engineered nanoparticles interacting with cells: size matters. J Nanobiotechnology. 2014;12:5. https://doi.org/10.1186/1477-3155-12-5.
49. Bezerra AG, Machado TN, Woiski TD, Turchetti DA, Lenz JA, Akcelrud L, et al. Plasmonics and SERS activity of post-transition metal nanoparticles. J Nanopart Res. 2018;20:142. https://doi.org/10.1007/s11051-018-4249-8.
50. Fröhlich E. The role of surface charge in cellular uptake and cytotoxicity of medical nanoparticles. Int J Nanomed. 2012;7:5577–91. https://doi.org/10.2147/ijn.s36111.